Talanta 85 (2011) 56–62

Contents lists available at ScienceDirect

Talanta

journal homepage: www.elsevier.com/locate/talanta

Electrogenerated chemiluminescence of anatase TiO_2 nanotubes film

Lifen Chen [a], Lili Lu [b], Yan Mo [a], Zemin Xu [a], Shunping Xie [c], Hongyan Yuan [b], Dan Xiao [a,b,*], Martin M.F. Choi [c,**]

[a] College of Chemistry, Sichuan University, Chengdu 610064, PR China
[b] College of Chemical Engineering, Sichuan University, Chengdu 610064, PR China
[c] Department of Chemistry, Hong Kong Baptist University, 224 Waterloo Road, Kowloon Tong, Hong Kong, China

ARTICLE INFO

Article history:
Received 6 October 2010
Received in revised form 1 March 2011
Accepted 8 March 2011
Available online 2 April 2011

Keywords:
Electrochemiluminescence
TiO_2
Nanotubes
Semiconductor
Sensor

ABSTRACT

Highly ordered titanium dioxide (TiO_2) nanotubes film was successfully synthesized via anodic oxidation of a Ti foil in an ammonium fluoride-based ethylene glycol solution. The electrogenerated chemiluminescence (ECL) behavior of the resulting TiO_2 nanotubes film was subsequently studied. Strong ECL emission was observed at −1.40 V (vs. Ag/AgCl) and the ECL spectrum displayed three emission peaks which were bathochromatically shifted by ca. 140 nm as compared to its corresponding photoluminescence (PL) emission peaks, indicating that the surface state plays an important role in the emission process. The ECL emission can also occur in a deareated solution attributing to the surface adsorbed O_2 molecules. The ECL emission intensity was quenched by dopamine and greatly enhanced in the presence of dissolved O_2 and H_2O_2, making it possible to detect these analytes. The TiO_2 nanotubes film has been successfully applied to determine the dissolved O_2 content in river and pond water samples, the H_2O_2 concentration in commercial disinfectant samples and the dopamine concentration in commercial dopamine injections with satisfactory results. The plausible ECL mechanisms of TiO_2 nanotubes film in aqueous solution are discussed.

1. Introduction

Semiconductor nanocrystals (NCs) have recently attracted intensive attentions due to their unique size- and shape-dependent electrochemical, electronic, magnetic and optical properties [1–5]. The electrogenerated chemiluminescence (ECL) behavior of NCs, which has great potential in novel ECL sensors and biological labels for ECL detection, has been widely studied in recent years after Bard and his co-workers firstly reported the ECL of silicon quantum dots (Si QDs) [6]. Subsequently, the ECL behaviors of CdSe NCs [7], CdSe/ZnSe NCs [8], Ge NCs [9], CdTe NCs [10], and PbS NCs [11] in organic solvents, and CdSe NCs [12], CdSeTd/ZnS NCs [13], CdTe NCs [14], and CdS nanotubes [15] in aqueous systems were investigated.

As a wide-band-gap semiconductor material, titanium dioxide (TiO_2) is one of the most important transition metal oxides. Since Fujishima and Honda first discovered that single-crystal TiO_2 semiconductor is highly active for the photocatalytic decomposition of H_2O in 1972 [16], it has been extensively delved in the fields of environmental purification and solar energy conversion [17–21]. TiO_2 can be fabricated in various nanostructures. The highly ordered TiO_2 nanotubes can offer larger surface area without sacrificing the geometric and structural order, maintain uniform pore-size distribution and possess favorable charge-transport properties [22]. In addition, it entails a larger number of active reaction sites for chemical reactions to take place. As such, it has been widely studied due to its geometric features of unique photoelectronics and photocatalysis properties. For instances, TiO_2 nanotubes have been used in synthesizing dye-sensitized solar cells [22–24], opto-electronic devices [24], water-photoelectrolysis system [25], photocatalyst [26], gas sensors [27,28] and is an anode material for lithium-ion batteries [29]. Moreover, TiO_2 is nontoxic, biocompatible and environmentally safe; and has been used in biomedical field such as drug delivery and release [26,30] and as a substrate for immobilizing biomolecules [31]. Some interesting photo- and electro-luminescence behaviors of TiO_2 have also been reported [32–34] but its ECL behavior has not been widely studied. Although the ECL characteristic of TiO_2/Nafion in aqueous solution using linear sweep voltammetry and the ECL of Ag/TiO_2 nanotubes using $S_2O_8^{2-}$ as a coreactant was recently investigated [35,36], the ECL of TiO_2 nanotubes film using cyclic voltammetry (CV) without coreactant has never been reported.

In this work, the electrochemical and ECL behaviors of TiO_2 nanotubes film in aqueous potassium nitrate (KNO_3) solution were

* Corresponding author at: College of Chemistry, Sichuan University, Chengdu 610064, PR China. Tel.: +86 28 85415029; fax: +86 28 85416029.
** Corresponding author. Tel.: +852 34117839; fax: +852 34117348.
E-mail addresses: xiaodan@scu.edu.cn (D. Xiao), mfchoi@hkbu.edu.hk (M.M.F. Choi).

0039-9140/$ – see front matter © 2011 Elsevier B.V. All rights reserved.
doi:10.1016/j.talanta.2011.03.011

studied using CV. It was found that the TiO_2 nanotubes film display some favorable ECL properties. The vertically oriented TiO_2 nanotubes exhibit three emission peaks in the ECL spectrum which are bathochromatically shifted as compared to its photoluminescence (PL) spectrum. The main attribute of our TiO_2 nanotubes film is that it can produce stable and reproducible ECL signal in deareated solutions with no added coreactant. On the other hand, the ECL intensity can be greatly enhanced by coreactants such as dissolved O_2 and H_2O_2.

The determination of dopamine is of great importance in biochemistry. Several electrochemical methods using TiO_2 for analysis of dopamine have been developed [37]. Nevertheless, not much attention has been paid to determine dopamine using TiO_2 nanotubes film based on ECL. In this work, we attempt to use our TiO_2 nanotubes film to determine dopamine at low concentrations. Finally, the plausible ECL mechanisms of TiO_2 nanotubes film in aqueous solution are proposed. Compared with the previously reported ECL system [35], our self-organized TiO_2 nanotubes film possesses the advantages of ease of fabrication, excellent photo- and ECL-stability. In addition, our proposed ECL technique has been successfully applied to determine dissolved O_2, H_2O_2 and dopamine in real samples. The experimental results demonstrate that it can be utilized in developing simple and sensitive ECL methods for detection of these analytes.

2. Experimental

2.1. Chemicals

Potassium nitrate and ammonium persulfate were purchased from Sinopharm Chemical Reagent Company (Shanghai, China). Ammonium fluoride was obtained from Chengdu Chemicals (Sichuan, China) and ethylene glycol was from Meilin Industry and Trade Co., Ltd. (Tianjin, China). Hydrogen peroxide was purchased from Kelong Chemical Reagent Company (Sichuan, China). Dopamine was obtained from Sigma–Aldrich (St. Louis, MO, USA). All reagents of analytical purity were used as received without further purification. Double-distilled water was used throughout the experiments.

2.2. Apparatus

Electrochemical measurements were performed in a conventional three-electrode system in which a bare Ti foil or TiO_2 nanotubes film (10 mm × 10 mm) was employed as the working electrode, a 0.5-mm diameter platinum (Pt) wire and an Ag/AgCl (saturated with KCl) electrode were used as the counter and reference electrodes, respectively. The ECL signals were obtained from an MPI-E electrochemiluminescence analyzer system (Xi'an Remax Analyse Instrument Co., Ltd., Xi'an, China). The working voltage of the photomultiplier tube was 800 V. The PL spectrum was acquired on a Hitachi F-4500 fluorescence spectrophotometer (Tokyo, Japan) with a Xe lamp as the excitation light source. The ECL spectrum was constructed by plotting the ECL intensity of the TiO_2 nanotubes film against the cut-on wavelengths (400, 425, 440, 460, 490, 504, 535, 555, 575, 588, 606, 620, and 640 nm) of a series of optical filters used. X-ray diffraction (XRD) measurements were performed on a Tongda TD-3500 X-ray powder diffractometer (Liaoning, China) with Cu Kα radiation (λ = 0.154 nm). The XRD patterns were recorded from 20° to 80° at a scan rate of 0.06°/s. The morphologies of TiO_2 nanotubes film were examined using a Hitachi S-4800 ultra-high resolution field emission scanning electron microscope (Tokyo, Japan). The Brunauer–Emmett–Teller (BET) surface area of TiO_2 nanotubes film was determined by nitrogen (N_2) adsorption method using a Quadrasorb^{TM} *SI* Surface Area and Pore Size Analyzer (Quantachrome, Instruments, Boynton Beach, FL, USA). Infrared (IR) absorption spectra of the KBr disks containing powder samples were recorded on a Nicolet 6700 FT-IR spectrometer (Thermo Scientific, Sugar Land, TX, USA) at a resolution of 4 cm^{-1} in the range of 400–4000 cm^{-1}.

2.3. Preparation of TiO_2 nanotubes film

The TiO_2 nanotubes film was synthesized according to a previously reported method [38]. A Ti foil (99.6% purity) was sonicated in acetone, isopropanol and double-distilled water successively, followed by drying in a stream of N_2 prior to the electrochemical treatment. The Ti foil was anodized at a constant potential of 60 V for 10 h in a ethylene glycol solution of 0.05% NH_4F using a Pt wire as the counter electrode at room temperature. After anodization, the Ti foil was ultrasonically cleaned in double-distilled water to remove surface debris and dried in a stream of N_2. The resulting TiO_2 nanotubes film was then sintered at 450 °C in air for 2 h and then cooled to room temperature.

2.4. Sample preparation

Pond water river water samples were collected from the campus pond and Jin River, respectively. Before ECL measurement, the water samples were added with KNO_3 as the supporting electrolyte to a final concentration of 0.10 M. Two different commercial H_2O_2 disinfectants were purchased from a local drugstore and two different brands of dopamine hydrochloride injections were obtained from a local hospital. The H_2O_2 and the dopamine samples were diluted with appropriate volumes of double-distilled water prior to the ECL measurement.

3. Results and discussion

3.1. Synthesis and characterization

The highly ordered TiO_2 nanotubes film was synthesized by an anodic oxidation of Ti foil in a NH_4F-based ethylene glycol solution. The top surface and cross-section morphology of the nanotubes film was studied by SEM as depicted in Fig. 1a–c. The SEM images show that the TiO_2 nanotubes with an average inner diameter of ~80 nm, ~15 nm thickness and ~1 μm length were aligned orderly on the surface of the Ti foil. The BET surface area of the nanotubes film was determined as 43.21 m^2/g. Fig. 1d compares the XRD patterns of the film with and without annealing at 450 °C for 2 h. It is obvious that the anodized TiO_2 film is almost entirely amorphous (1) but can be converted into anatase-structure (2) after annealing at 450 °C. Our results indicate that annealing TiO_2 is an essential step to obtain well-organized TiO_2 nanotubes on the Ti foil. The XPS spectrum of TiO_2 nanotubes film was also acquired which clearly shows the presence of Ti 2p and O 1s on the Ti foil (Fig. S1 of Supplementary Data).

3.2. PL and ECL spectra of the TiO_2 nanotubes film

Fig. 2 displays the (a) photoluminescence (PL) and (b) ECL spectra of the TiO_2 nanotubes film. The PL spectrum was acquired at an excitation wavelength of 261 nm. The ECL spectrum was obtained by collecting the ECL data during CV potential sweep with the use of a series of optical filters (cut-on wavelengths: 400, 425, 440, 460, 490, 504, 535, 555, 575, 588, 606, 620, and 640 nm). The ECL spectrum is bathochromically shifted as compared to the PL spectrum. The PL spectrum possesses two emission peaks at around 414 and 472 nm accompanied by four shoulder peaks at ca. 370, 454, 484, and 495 nm (Fig. 2a). Three emission peaks at ca. 510, 554 and 606 nm are observed for the ECL spectrum (Fig. 2b). It is obvious

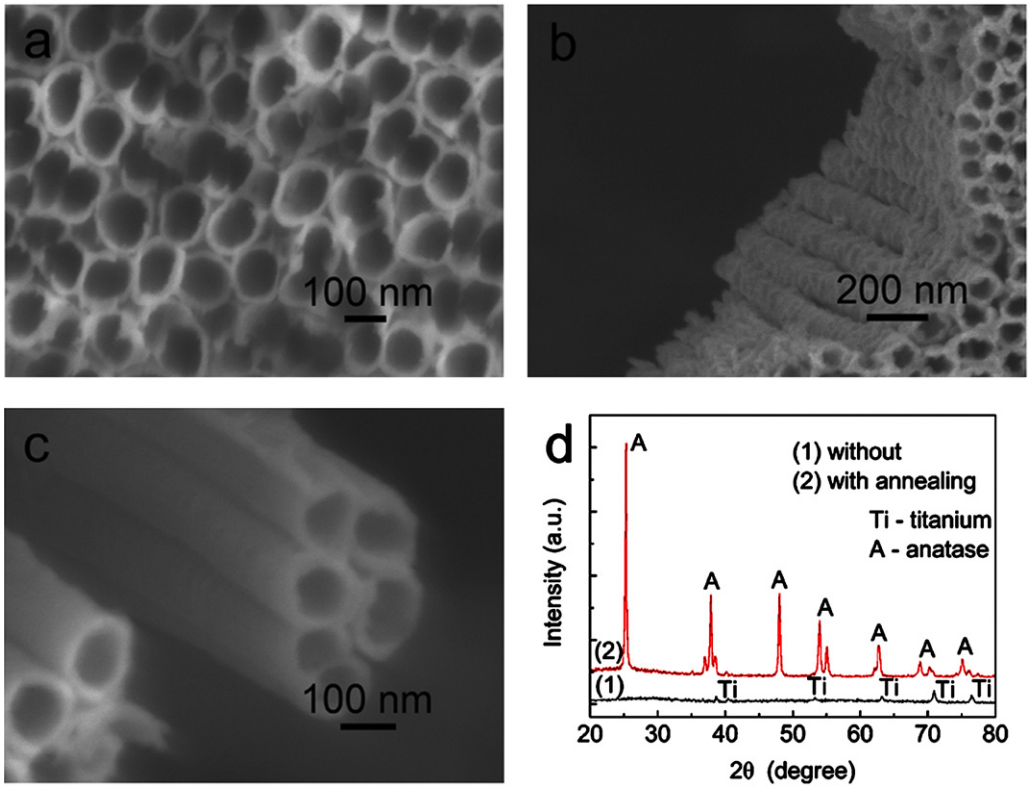

Fig. 1. SEM images of the (a) top surface, (b) cross-sections with lower and (c) higher magnifications of TiO_2 nanotubes film. (d) XRD patterns of Ti film samples without and with annealing at 450 °C for 2 h. A and Ti are anatase and titanium peaks, respectively.

that the energy states of the photo-excited TiO_2 are different quite from that of the electro/chemo-generated excited TiO_2.

The PL emission peak at 370 nm is proposed to be ascribed to the energy vertical transitions at the X edge of the Brillouin zone: $X_{1a} \rightarrow X_{1b}$ [39,40] and the 415 nm band in our case may attribute to the lowest energy indirect transitions from the edge to the center of the Brillouin zone, $X_{1a} \rightarrow \Gamma_{1b}$, which is close to the transition energy diagrams of TiO_2 particles calculated by Daude et al. [40]. In addition, the PL measurements reveal that the presence of four peaks at 454, 472, 484, and 495 nm might arise from the electron transition mediated by defect levels such as oxygen vacancies in the band gap at various energies [41]. The ECL peaks are red-shifted by ca. 140 nm as compared to the corresponding PL peaks which is consistent with the previous work of Si [6], CdSe [7] and Ge [9], suggesting that the surface state of TiO_2 nanotubes plays an important role in the electrochemical and emission processes.

3.3. *ECL behavior of TiO_2 nanotubes film*

Cyclic voltammetry, which can provide definite redox reactions, was employed to characterize the ECL behavior and emission stability of the TiO_2 nanotubes film. Fig. 3a shows the CV and ECL curves of a Ti foil in 0.10 M KNO_3 solution (pH 5.6) at a scan rate of 0.10 V/s. No ECL light emission was detected and the background current was very low. However, when a TiO_2 nanotubes film was used, under the same CV conditions, the cathodic current was greatly increased and the ECL signal was strong with a maximum of −1.40 V in the negative scan (Fig. 3b), suggesting that these ECL phenomena must have derived from the TiO_2 nanotubes. It was also found that the light emission intensity of the TiO_2 nanotubes film was higher at the more positive scan potential windows as depicted in Fig. S2, possibly attributing to the oxygen effect derived from the decomposition of water or more charge injections. As such, the ECL emission was conducted at a negative potential scan of 0.0 to −1.6 V to preclude these effects. The ECL peaks under the negative potentials indicate that TiO_2 nanotubes are reduced to $TiO_2^{\bullet -}$ which can subsequently react with some oxidized species or some coreactants to produce excited-states TiO_2^* and then decay back to its ground state with a concomitant release of luminescence (*vide infra*).

In addition, TiO_2 can exist as rutile-phase. Thus, the ECL of the rutile-phase TiO_2 nanotubes film was investigated. The TiO_2 nanotubes film turned to rutile-phase structure after annealing at 900 °C for 2 h. Fig. S3 displays its XRD pattern. Similar CV and ECL experiments were conducted on the rutile-phase TiO_2 nanotubes film (Fig. S4). It was found that light emission started to appear at −1.30 V and gradually increased with the negative potential scan. Unfortunately, its ECL intensity is 2.5 times lower than that of anatase-phase TiO_2 nanotubes film. Thus, we only focus our studies on anatase-phase TiO_2 nanotubes film in the subsequent work.

The effect of dissolved O_2 on ECL intensity was investigated and displayed in Fig. 4. Various concentrations of O_2 (balanced with N_2) gases were bubbled through the 0.10 M KNO_3 solution (pH 5.6). CV scan was then applied and the ECL of anatase-phase TiO_2 nanotubes film was monitored. The ECL intensity increased with the increase in dissolved O_2, inferring that O_2 plays an important role in enhancing the ECL reactions of TiO_2 nanotubes film. The ECL emission intensity increases linearly over the range 20–80% O_2 solution (correlation coefficient of 0.9979, the inset in Fig. 4). This optical response might be attributed in part to the trapping of electrons in surface states during the CV [42] and the adsorption of O_2 molecules during the ECL process. In order to further investigate the oxygen effect on ECL processes, H_2O_2 was added into the deareated electrolyte and the ECL is shown in Fig. S5. The ECL intensity was enhanced in the presence of H_2O_2. The ECL reaction mechanisms can thus be summarized according to these results and other previous reports [12,43]:

$$TiO_2 + e^- \rightarrow TiO_2^{\bullet -} \quad (1)$$

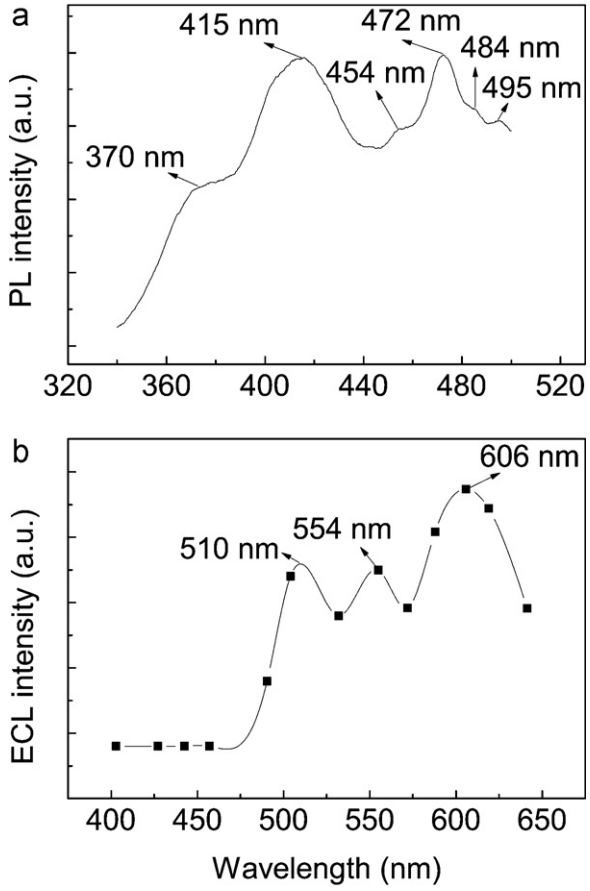

Fig. 2. (a) PL and (b) ECL spectra of the TiO_2 nanotubes film in 0.10 M KNO_3 (pH 5.6). The PL spectrum was acquired at an excitation wavelength of 261 nm. The ECL spectrum was obtained by plotting the ECL intensity against the cut-on wavelength of the optical filter used to capture the ECL intensity under CV scan between 0.0 and −1.60 V at 0.10 V/s.

$$O_2 + H_2O + 2e^- \rightarrow OOH^- + OH^- \quad (2)$$

$$2TiO_2^{\bullet -} + OOH^- + H_2O \rightarrow 3OH^- + 2TiO_2^* \quad (3)$$

or

$$2TiO_2^{\bullet -} + H_2O_2 \rightarrow 2OH^- + 2TiO_2^* \quad (4)$$

$$TiO_2^* \rightarrow TiO_2 + h\upsilon \quad (5)$$

Initially, the TiO_2 nanotubes film is reduced to $TiO_2^{\bullet -}$ by charge injection during the negative potential scan (Eq. (1)). The dissolved O_2 is also simultaneously reduced to OOH^- (Eq. (2)) which can then act as a coreactant to react with $TiO_2^{\bullet -}$ to form the excited state TiO_2^* (Eq. (3)). When the excited state TiO_2^* falls back to its ground state TiO_2, photon will be released (Eq. (5)). Similarly, H_2O_2 in the solution can directly react with $TiO_2^{\bullet -}$ to produce the excited state TiO_2^* (Eq. (4)) with a concomitant release of photon (Eq. (5)).

It is interesting to note that weak ECL could still be observed after the electrolyte was deareated by a stream of high-purity N_2 for more than 40 min (Fig. 4a) which is quite different from the literature results [35]. The ECL mechanism of TiO_2 nanotubes film in a deareated solution can be explained as follows: there are lots of oxygen vacancies and defects on the surface of TiO_2 nanotubes and the applied potentials facilitate the formation of more available holes [44]. Moreover, the unique structure of the highly ordered TiO_2 nanotube arrays allows fast and efficient transfer of electrons. These are all factors that can make surface oxygen vacancies and defects bind with electrons easily to form the excited state in the sub-band, thus, light emission can still occur after deaeration. This

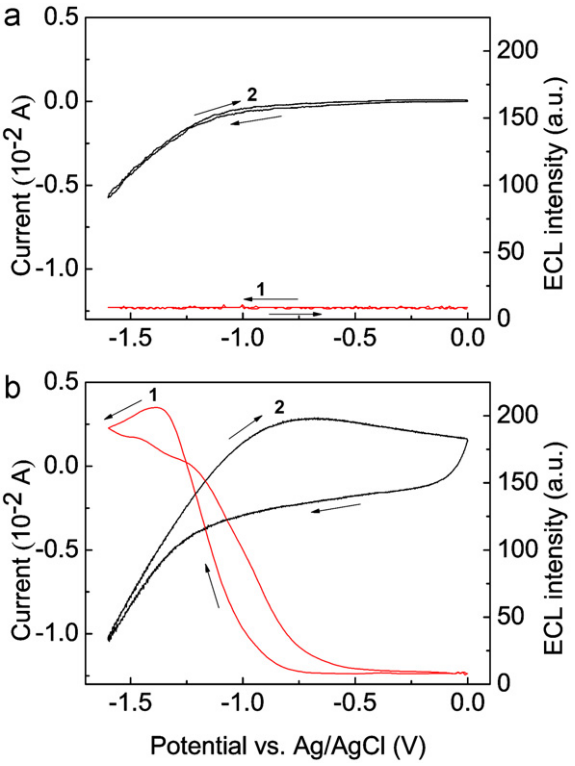

Fig. 3. ECL (curve 1) and CV (curve 2) curves of (a) Ti foil and (b) TiO_2 nanotubes film in 0.10 M KNO_3 solution (pH 5.6) with the potential cycled from 0.0 to −1.60 V at a scan rate of 0.10 V/s.

may also be attributed to the initial adsorption of O_2 molecules on the surface of TiO_2 nanotubes due to its large surface-to-volume ratio. The ECL mechanisms of the TiO_2 nanotubes film in both deareated and O_2-saturated solutions are summarized in Scheme 1. The inset of Fig. 4 shows that the ECL intensity starts to level off at higher O_2 concentration (>80%) probably due to the fact that the O_2 molecules have already been fully occupied on the TiO_2 nanotubes surface so that further increase in O_2 has no effect on ECL.

The effect of scan rate on the ECL intensity was studied and shown in Fig. 5. The ECL intensity increased sharply with the increase in scan rate at 0.020–0.10 V/s and then slowly at 0.10–0.20 V/s. The increase in ECL emission is probably related to the diffusion of the oxidized species at the surface of the electrode, *i.e.*, the higher the scan rate, the easier the ECL reactions to

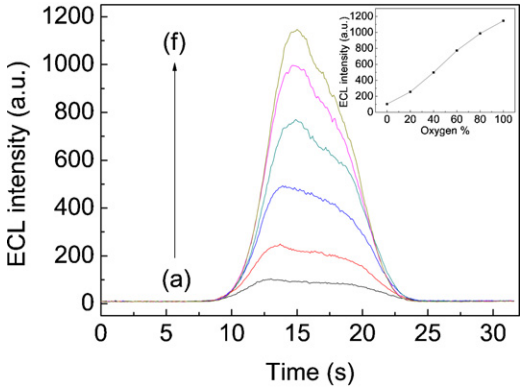

Fig. 4. ECL emission intensities of TiO_2 nanotubes film in 0.10 M KNO_3 solution (pH 5.6) saturated with different % of O_2 gases: (a) 0.0, (b) 20, (c) 40, (d) 60, (e) 80, and (f) 100%. The potential cycled from 0.0 to −1.60 V at a scan rate of 0.10 V/s. The inset displays the plot of ECL response of the TiO_2 nanotubes film against % of O_2.

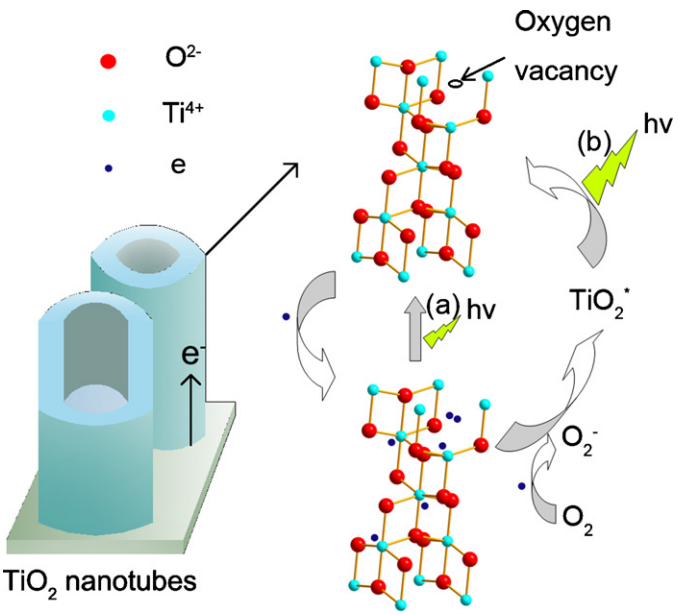

Scheme 1. Schematic diagram illustrates the ECL mechanisms of the TiO_2 nanotubes film in both (a) deareated and (b) O_2-saturated solutions.

take place. In other words, ECL is prone to the diffusion-controlled process.

It is well-known that the ECL of semiconductor NCs is sensitive to pH. The effect of pH on the ECL of TiO_2 nanotubes film was investigated and depicted in Fig. 6. The ECL intensity increases with the increase in pH 3.0–5.6 and then declines with further increase in pH 5.6–10. Maximum ECL intensity is obtained under mild acidic conditions, suggesting that small quantities of H^+ in the electrolyte solution can enhance the light emission. However, in strong acidic conditions, the excess protons will be electro-adsorbed at the band edge trap sites of TiO_2 (Eq. (6)) resulting in inhibition of ECL [45].

$$TiO_2 + H^+ + e^- \rightarrow TiO(OH) \quad (6)$$

On the other hand, the ECL intensity drops in the basic conditions, attributing to the fact that high concentration of OH^- will inhibit the formation of OOH^- (Eq. (2)). As a result, weak ECL emission was observed.

Dopamine is an important neurotransmitter which plays a significant role in the central nervous, renal, hormonal and cardiovascular system. It has been reported that the two hydroxyl groups in the ortho position of dopamine can chelate with the surface Ti atoms, resulting in a five-membered ring coordination complex

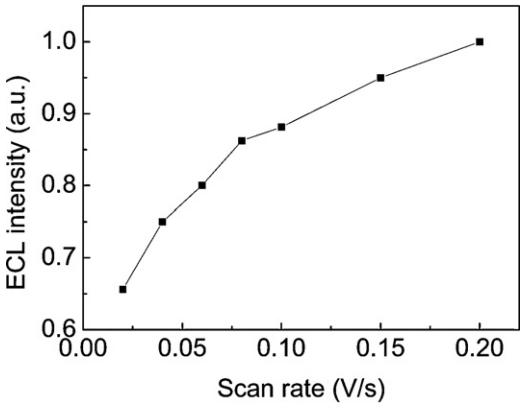

Fig. 5. Effect of scan rate on the ECL intensity of TiO_2 nanotubes film in 0.10 M KNO_3 solution (pH 5.6) with the potential cycled from 0.0 to −1.60 V.

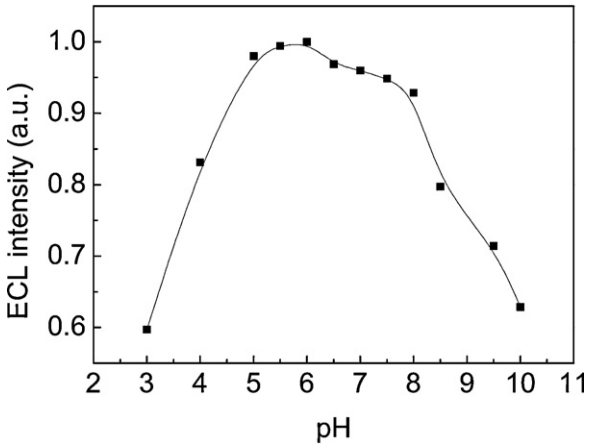

Fig. 6. Effect of pH on the ECL intensity of the TiO_2 nanotubes film in 0.10 M KNO_3 solutions under various pHs. The potential was cycled from 0.0 to −1.60 V at a scan rate of 0.10 V/s.

[46]. In the present work, dopamine was introduced into the solution to study its effect on the ECL of TiO_2 nanotubes film. Fig. 7 displays the ECL intensities of the TiO_2 nanotubes film in 0.10 M KNO_3 solution (pH 5.6) in the presence of various concentrations of dopamine. The ECL intensity was monotonic decreased with the increase in concentration of dopamine and almost completely quenched by 3.0 mM dopamine. This result might be ascribed to the chelation of the enediol moiety of dopamine with the surface Ti atoms, thus inhibiting the reaction between TiO_2 and other oxidized species. The formation of dopamine-Ti complex at the surface of the TiO_2 nanotubes film is confirmed by FTIR studies. Fig. 8 depicts the IR spectra of the TiO_2 nanotubes film before and after exposure to dopamine. Both spectra display the broad band at around 3400 cm^{-1}, corresponding to the surface adsorbed water and hydroxyl groups. Another typical broad band between 400 and 900 cm^{-1} is originated from the Ti–O–Ti band of TiO_2. However, there are some obvious differences in the IR spectra between the TiO_2 nanotubes (Fig. 8a) and dopamine adsorbed TiO_2 nanotubes (Fig. 8b) samples. A significant increase of the absorption signal at ~1631 cm^{-1} appears in the dopamine adsorbed TiO_2 nanotubes sample, attributing to the O–H bending of the adsorbed water plus N–H bending and C=C ring stretching vibration of dopamine [47,48]. In addition, the bands at ~1486 and 1398 cm^{-1} can be assigned to the benzene ring stretching whereas the band at ~1273 cm^{-1} is C–O stretching. A new band at 1073 cm^{-1} ascribing to the aryl-oxygen stretching vibration is also observed for

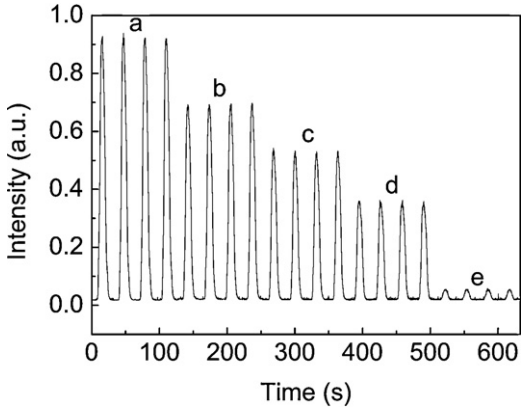

Fig. 7. ECL emission intensities of TiO_2 nanotubes film in 0.10 M KNO_3 solution (pH 5.6) with various concentrations of dopamine (a) 0.00, (b) 5.00, (c) 10.0, (d) 100, and (e) 3000 μM. The potential cycled from 0.0 to −1.60 V at a scan rate of 0.10 V/s.

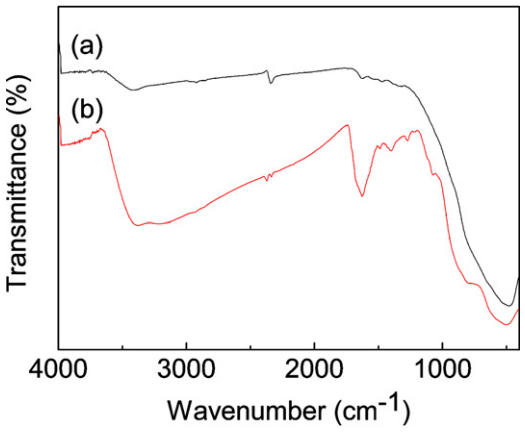

Fig. 8. FTIR spectra of TiO_2 nanotubes film (a) before and (b) after exposure to dopamine.

the dopamine adsorbed TiO_2 nanotubes sample. All these results clearly show that dopamine binds to the oxide surfaces in a bidentate dianion form [49]. As such, it is possible to develop a new ECL method based on TiO_2 nanotubes for the determination of dopamine. It is anticipated that other compounds such as ascorbic acid, epinephrine and norepinephrine containing enediol moieties will also behave similarly. In essence, it is possible to develop a high-performance liquid chromatographic method in conjunction with the use of our TiO_2 nanotubes for detection of these analytes.

3.4. Real sample analysis

In order to investigate the feasibility of the TiO_2 nanotubes film electrode for analyzing real samples, the dissolved O_2 content in environmental water samples, the H_2O_2 concentration of disinfectants and the dopamine concentration of injection samples were examined using our proposed ECL method. The results are summarized in Table 1. The recoveries range from 96.0% to 106%, indicating that the proposed TiO_2 nanotubes film electrode can be applied to real sample analysis.

Table 1
Determination of dissolved O_2, H_2O_2 and dopamine in real samples.

Analyte	Sample	Added concentration	Found concentration	Recovery (%)
Dissolved O_2	Pond water	–	10.1 mg/L	–
		6.78 mg/L[a]	6.63 mg/L	97.8
		4.52 mg/L[a]	4.48 mg/L	99.2
		2.26 mg/L[a]	2.36 mg/L	104
	River water	–	8.02 mg/L	–
		6.78 mg/L[a]	6.88 mg/L	101
		4.52 mg/L[a]	4.63 mg/L	102
		2.26 mg/L[a]	2.23 mg/L	98.5
H_2O_2	Sample 1	–	0.84 M	–
		1.00 M	1.87 M	103
		1.00 M	1.87 M	103
	Sample 2	–	0.98 M	–
		1.00 M	1.94 M	96.0
		1.00 M	2.03 M	105
Dopamine	Sample 1	–	51.0 mM	–
		50.0 mM	104 mM	106
		50.0 mM	102 mM	102
	Sample 2	–	52.0 mM	–
		50.0 mM	102 mM	100
		50.0 mM	101 mM	98.0

[a] The water samples were bubbled by a stream of 15%, 10% and 5% v/v O_2 balanced with N_2, respectively, at 18 °C.

4. Conclusion

In summary, highly ordered TiO_2 nanotubes film was prepared by anodic oxidation in a NH_4F-based ethylene glycol solution. This well-organized TiO_2 nanotubes film possesses the advantages of ease of fabrication and good stability. It displays stable, strong and reproducible ECL emission in aqueous solution. Maximum ECL emission occurs at −1.40 V, indicating that TiO_2 nanotubes film is reduced to $TiO_2^{\bullet-}$ and then react with some oxidized species or coreactants including O_2, H_2O_2 and $(NH_4)_2S_2O_8$ (Fig. S6) to form the excited-states TiO_2^*. Light emission is produced when TiO_2^* returns to its ground state. It was also found that ECL emission could still occur in deareated solution attributing to the surface defects and adsorption of O_2 molecules on the TiO_2 nanotubes surface. Besides, the ECL signal can be inhibited by dopamine possibly due to the formation of a stable five-membered ring in the Ti and dopamine complex. The ECL spectrum was found to be red-shifted as compared to its PL spectrum, indicating that the surface state of TiO_2 should play an important role in the ECL process. Finally, the TiO_2 nanotubes film have been applied to determine the concentrations of dissolved O_2, H_2O_2 and dopamine in real samples with satisfactory results.

Acknowledgements

Financial supports from the National Nature Science Foundation of China (20927007) and Youth Foundation of Sichuan University (No. 2010SCU11048) are gratefully acknowledged. We also express sincere thanks to Professor Yi Lv (School of Chemistry, Sichuan University) for his helpful discussion.

Appendix A. Supplementary data

Supplementary data associated with this article can be found, in the online version, at doi:10.1016/j.talanta.2011.03.011.

References

[1] M. Bruchez Jr., M. Moronne, P. Gin, S. Weiss, A.P. Alivisatos, Science 281 (1998) 2013–2016.
[2] W.C.W. Chan, S.M. Nie, Science 281 (1998) 2016–2018.
[3] Y.D. Yin, A.P. Alivisatos, Nature 437 (2005) 664–670.
[4] M.Y. Han, X.H. Gao, J.Z. Su, S.M. Nie, Nat. Biotechnol. 19 (2001) 631–635.
[5] C. Burda, X.B. Chen, R. Narayanan, M.A. El-Sayed, Chem. Rev. 105 (2005) 1025–1102.
[6] Z.F. Ding, B.M. Quinn, S.K. Haram, L.E. Pell, B.A. Korgel, A.J. Bard, Science 296 (2002) 1293–1297.
[7] N. Myung, Z.F. Ding, A.J. Bard, Nano Lett. 2 (2002) 1315–1319.
[8] N. Myung, Y. Bae, A.J. Bard, Nano Lett. 3 (2003) 1053–1055.
[9] N. Myung, X.M. Lu, K.P. Johnston, A.J. Bard, Nano Lett. 4 (2004) 183–185.
[10] Y. Bae, N. Myung, A.J. Bard, Nano Lett. 4 (2004) 1153–1161.
[11] L.F. Sun, L. Bao, B.R. Hyun, A.C. Bartnik, Y.W. Zhong, J.C. Reed, D.W. Pang, H.D. Abruña, G.G. Malliaras, F.W. Wise, Nano Lett. 9 (2009) 789–793.
[12] G.Z. Zou, H.X. Ju, Anal. Chem. 76 (2004) 6871–6876.
[13] G.X. Liang, L.L. Li, H.Y. Liu, J.R. Zhang, C. Burda, J.J. Zhu, Chem. Commun. 46 (2010) 2974–2976.
[14] Y. Wang, J. Lu, L.H. Tang, H.X. Chang, J.H. Li, Anal. Chem. 81 (2009) 9710–9715.
[15] Y.M. Fang, J.J. Sun, A.H. Wu, X.L. Su, G.N. Chen, Langmuir 25 (2009) 555–560.
[16] A. Fujishima, K. Honda, Nature 38 (1972) 37–38.
[17] M. Grätzel, Nature 414 (2001) 338–344.
[18] U. Bach, D. Lupo, P. Comte, J.E. Moser, F. Weissörtel, J. Salbeck, H. Spreitzer, M. Grätzel, Nature 395 (1998) 583–585.
[19] D. Mitoraj, H. Kisch, Angew. Chem. Int. Ed. 47 (2008) 9975–9978.
[20] A. Wolcott, W.A. Smith, T.R. Kuykendall, Y.P. Zhao, J.Z. Zhang, Small 5 (2009) 104–111.
[21] W. Zhu, X. Liu, H.Q. Liu, D.L. Tong, J.Y. Yang, J.Y. Peng, J. Am. Chem. Soc. 132 (2010) 12619–12626.
[22] K. Zhu, N.R. Neale, A. Miedaner, A.J. Frank, Nano Lett. 7 (2007) 69–74.
[23] J. Wang, Z.Q. Lin, Chem. Mater. 22 (2010) 579–584.
[24] K. Shankar, J. Bandara, M. Paulose, H. Wietasch, O.K. Varghese, G.K. Mor, T.J. LaTempa, M. Thelakkat, C.A. Grimes, Nano Lett. 8 (2008) 1654–1659.
[25] G.K. Mor, K. Shankar, M. Paulose, O.K. Varghese, C.A. Grimes, Nano Lett. 5 (2005) 191–195.

[26] N.K. Shrestha, J.M. Macak, F. Schmidt-Stein, R. Hahn, C.T. Mierke, B. Fabry, P. Schmuki, Angew. Chem. Int. Ed. 48 (2009) 969–972.
[27] O.K. Varghese, D.W. Gong, M. Paulose, K.G. Ong, C.A. Grimes, Sens. Actuators B 93 (2003) 338–344.
[28] H.F. Lu, F. Li, G. Liu, Z.G. Chen, D.W. Wang, H.T. Fang, G.Q. Lu, Z.H. Jiang, H.M. Cheng, Nanotechnology 19 (2008) 405504–405510.
[29] J.W. Xu, C.H. Jia, B. Cao, W.F. Zhang, Electrochim. Acta 52 (2007) 8044–8047.
[30] K.C. Popat, M. Eltgroth, T.J. LaTempa, C.A. Grimes, T.A. Desai, Small 3 (2007) 1878–1881.
[31] Y.Y. Song, F. Schmidt-Stein, S. Bauer, P. Schmuki, J. Am. Chem. Soc. 131 (2009) 4230–4232.
[32] S.K. Poznyak, A.I. Kulak, Talanta 43 (1996) 1607–1613.
[33] B. Smandek, H. Gerischer, Electrochim. Acta 34 (1989) 1411–1415.
[34] S.K. Poznyak, A.I. Kulak, Sens. Actuators B 22 (1994) 97–100.
[35] Z.Y. Lin, Y. Liu, G.N. Chen, Electrochem. Commun. 10 (2008) 1629–1632.
[36] J.X. Li, L.X. Yang, S.L. Luo, B.B. Chen, J. Li, H.L. Lin, Q.Y. Cai, S.Z. Yao, Anal. Chem. 82 (2010) 7357–7361.
[37] M. Mazloum-Ardakani, H. Rajabi, H. Beitollahi, B.B.F. Mirjalili, A. Akbari, N. Taghavinia, Int. J. Electrochem. Sci. 5 (2010) 147–157.
[38] W.T. Sun, Y. Yu, H.Y. Pan, X.F. Gao, Q. Chen, L.M. Peng, J. Am. Chem. Soc. 130 (2008) 1124–1125.
[39] N. Serpone, D. Lawless, R. Khairutdinov, J. Phys. Chem. 99 (1995) 16646–16654.
[40] N. Daude, C. Gout, C. Jouanin, Phys. Rev. B 15 (1977) 3229–3235.
[41] J.X. Xu, L.P. Li, Y.J. Yan, H. Wang, X.X. Wang, X.Z. Fu, G.S. Li, J. Colloid Interface Sci. 318 (2008) 29–34.
[42] G. Boschloo, D. Fitzmaurice, J. Phys. Chem. B 103 (1999) 2228–2231.
[43] L.J. Hua, H.Y. Han, H.B. Chen, Electrochim. Acta 54 (2009) 1389–1394.
[44] C.C. Sun, T.C. Chou, J. Mol. Catal. A: Chem. 151 (2000) 133–145.
[45] L.A. Lyon, J.T. Hupp, J. Phys. Chem. B 103 (1999) 4623–4628.
[46] T. Rajh, L.X. Chen, K. Lukas, T. Liu, M.C. Thurnauer, D.M. Tiede, J. Phys. Chem. B 106 (2002) 10543–10552.
[47] J.G. Yu, H.G. Yu, B. Cheng, X.J. Zhao, J.C. Yu, W.K. Ho, J. Phys. Chem. B 107 (2003) 13871–13879.
[48] T. Rajh, J.M. Nedeljkovic, L.X. Chen, O. Poluektov, M.C. Thurnauer, J. Phys. Chem. B 103 (1999) 3515–3519.
[49] P.A. Connor, K.D. Dobson, A.J. McQuillan, Langmuir 11 (1995) 4193–4195.